Medial prefrontal activity during delay period contributes to learning of a working memory task

Ding Liu *et al.*

Science **346**, 458 (2014);
DOI: 10.1126/science.1256573

the dense packing above the β face of the corrin ring (fig. S4A). The same steric constraints would disable an initial nucleophilic attack of Co^{I} on PCE. Instead, the short substrate-cofactor distances would allow the second electron transfer to occur either directly from the proximal [4Fe-4S] cluster or via the Co ion (Fig. 4). The strictly conserved Tyr^{246} is pointing with its phenolic hydroxyl group toward C1 and could donate the required proton to neutralize the carbanion (*20*). Deprotonation of Tyr^{246} could be stabilized by the neighboring positive charge of Arg^{305}. Equally, a role of Tyr^{246} in a radical route (*18*) cannot be excluded.

REFERENCES AND NOTES

1. C. Holliger, G. Wohlfarth, G. Diekert, *FEMS Microbiol. Rev.* **22**, 383–398 (1998).
2. B. Kräutler *et al.*, *Helv. Chim. Acta* **86**, 3698–3716 (2003).
3. L. A. Hug *et al.*, *Philos. Trans. R. Soc. London Ser. B* **368**, 20120322 (2013).
4. A. Mac Nelly, M. Kai, A. Svatoš, G. Diekert, T. Schubert, *Appl. Environ. Microbiol.* **80**, 4313–4322 (2014).
5. A. Neumann, G. Wohlfarth, G. Diekert, *J. Biol. Chem.* **271**, 16515–16519 (1996).
6. H. Scholz-Muramatsu, A. Neumann, M. Messmer, E. Moore, G. Diekert, *Arch. Microbiol.* **163**, 48–56 (1995).
7. Materials and methods are available on *Science* Online
8. T. Goris *et al.*, *Environ. Microbiol.* 10.1111/1462-2920.12589 (2014).
9. E. Miller, G. Wohlfarth, G. Diekert, *Arch. Microbiol.* **166**, 379–387 (1996).
10. L. Ye, A. Schilhabel, S. Bartram, W. Boland, G. Diekert, *Environ. Microbiol.* **12**, 501–509 (2010).
11. C. L. Drennan, S. Huang, J. T. Drummond, R. G. Matthews, M. L. Ludwig, *Science* **266**, 1669–1674 (1994).
12. F. Mancia *et al.*, *Structure* **4**, 339–350 (1996).
13. J. Kim, C. Gherasim, R. Banerjee, *Proc. Natl. Acad. Sci. U.S.A.* **105**, 14551–14554 (2008).
14. D. S. Froese *et al.*, *Biochemistry* **51**, 5083–5090 (2012).
15. H. B. Gray, J. R. Winkler, *Proc. Natl. Acad. Sci. U.S.A.* **102**, 3534–3539 (2005).
16. T. Svetlitchnaia, V. Svetlitchnyi, O. Meyer, H. Dobbek, *Proc. Natl. Acad. Sci. U.S.A.* **103**, 14331–14336 (2006).
17. M. John, R. P. H. Schmitz, M. Westermann, W. Richter, G. Diekert, *Arch. Microbiol.* **186**, 99–106 (2006).
18. J. Shey, W. A. van der Donk, *J. Am. Chem. Soc.* **122**, 12403–12404 (2000).
19. R. P. H. Schmitz *et al.*, *Environ. Sci. Technol.* **41**, 7370–7375 (2007).
20. G. Glod, W. Angst, C. Holliger, R. P. Schwarzenbach, *Environ. Sci. Technol.* **31**, 253–260 (1997).
21. W. Schumacher, C. Holliger, A. J. Zehnder, W. R. Hagen, *FEBS Lett.* **409**, 421–425 (1997).
22. K. M. McCauley *et al.*, *J. Am. Chem. Soc.* **127**, 1126–1136 (2005).

ACKNOWLEDGMENTS

H.D. acknowledges support by the Cluster of Excellence "Unifying Concepts in Catalysis (UniCat)." G.D. and T.S. were supported by the Deutsche Forschungsgemeinschaft (DFG) (Research Unit FOR 1530). M.B. was funded by the DFG through grant SFB 1078-A5. We are grateful for the funding of C.K. by the Ernst Abbe Foundation; in addition, we thank the staff at the Helmholtz-Zentrum Berlin (HZB) MX beamlines and DESY PETRA III beamline P11 for their assistance. We acknowledge access to beamlines of the BESSY II storage ring (Berlin, Germany) via the Joint Berlin MX-Laboratory. The authors thank O. Einsle for critical reading of the manuscript. Structure factors and models have been deposited in the Protein Data Bank under accession numbers 4UQU (empty), 4UR0 (TCE bound), 4UR1 (*cis*-DBE bound), 4UR2 (iodide bound), and 4UR3 ($P2_1$ crystal form).

SUPPLEMENTARY MATERIALS

www.sciencemag.org/content/346/6208/455/suppl/DC1
Materials and Methods
Figs. S1 to S6
Table S1
References (*23*–*35*)

30 June 2014; accepted 18 September 2014
Published online 2 October 2014;
10.1126/science.1258118

WORKING MEMORY

Medial prefrontal activity during delay period contributes to learning of a working memory task

Ding Liu,[1,2]* Xiaowei Gu,[1,2]* Jia Zhu,[1,2]* Xiaoxing Zhang,[1] Zhe Han,[1,2] Wenjun Yan,[1,2] Qi Cheng,[1,2] Jiang Hao,[1]† Hongmei Fan,[1] Ruiqing Hou,[1] Zhaoqin Chen,[1] Yulei Chen,[1] Chengyu T. Li[1]‡

Cognitive processes require working memory (WM) that involves a brief period of memory retention known as the delay period. Elevated delay-period activity in the medial prefrontal cortex (mPFC) has been observed, but its functional role in WM tasks remains unclear. We optogenetically suppressed or enhanced activity of pyramidal neurons in mouse mPFC during the delay period. Behavioral performance was impaired during the learning phase but not after the mice were well trained. Delay-period mPFC activity appeared to be more important in memory retention than in inhibitory control, decision-making, or motor selection. Furthermore, endogenous delay-period mPFC activity showed more prominent modulation that correlated with memory retention and behavioral performance. Thus, properly regulated mPFC delay-period activity is critical for information retention during learning of a WM task.

Working memory (WM) is essential for cognition by allowing active retention of behaviorally relevant information over a short duration known as the delay period (*1*–*3*). Previous studies have shown that the prefrontal cortex (PFC) is crucial for WM, because perturbation of PFC activity impaired WM (*3*) and WM-related activity was observed during the delay period in neurons of dorsal-lateral PFC (DL-PFC) in primates and medial PFC (mPFC) in rodents (*3*–*10*). Nevertheless, the functional role of PFC delay-period activity in WM remains unclear. Memory retention and attentional control are leading candidates (*2*, *3*, *11*). However, PFC is also critical for other brain functions (*3*, *12*, *13*) and has been suggested to be important for inhibitory control (*14*), decision-making (*15*), or motor selection (*16*). These roles cannot be distinguished by a delayed-response task, in which decision-making precedes the delay period (*3*, *12*). In addition, traditional methods for perturbing neural activity (*3*), including transcranial magnetic stimulation (*17*) and electrical stimulation (*18*), do not provide the temporal resolution and cell-type specificity required for delineating the functional role of PFC delay-period activity in WM. We addressed these issues by using a WM task with a delay period designed to temporally separate memory retention from other functions (*5*, *6*, *19*, *20*) and optogenetic approaches (*21*) to bidirectionally manipulate mPFC activity of excitatory and inhibitory neurons during the delay period.

Head-fixed mice were trained to perform an olfactory delayed nonmatch to sample (DNMS) task (Fig. 1, A and B; fig. S1; and movie S1), a modified version of the behavioral paradigms previously used in rats (*19*, *20*). For each trial, an olfactory stimulus (ethyl acetate, EA, or 2-pentanone, 2P) was presented as the sample, followed by a delay period (4 to 5 s) and then a testing olfactory stimulus, either matched or non-matched to the sample. Water-restricted mice were rewarded with water if they licked within a response time window in the nonmatch but not match trials (Fig. 1B and fig. S2). During the delay period, mice need to retain the information associated with the odor sample. The performance correct rate (referred to hereafter as performance), correct rejection rate, discriminability (d'), and lick efficiency steadily increased throughout the training, but there was a ceiling effect for the hit rate (Fig. 1, C and D, and fig. S3). The potential involvement of visual, auditory, or somatosensory cues was excluded (fig. S4A). The performance decreased with increasing duration of the delay period (fig. S4B), a typical hallmark of WM paradigms (*1*, *3*). For a genuine WM task, subjects should be able to perform beyond two cues (*19*, *20*), which was indeed observed (fig. S4C). We next expressed hM4Di, a designer receptor exclusively activated by designer drug (DREADD) (*22*), in mPFC with adeno-associated virus (AAV). Suppression of neural activity (fig. S5) by intraperitoneal injection of clozapine-N-oxide (CNO) significantly impaired the performance of the mice during the learning phase (days 1 to 5, Fig. 1E; statistics shown in table S1).

It is essential that mice were using WM instead of residual odor during the delay period to perform the task. Photoionization detector (PID)

[1]Institute of Neuroscience and Key Laboratory of Primate Neurobiology, Shanghai Institutes for Biological Sciences, Chinese Academy of Sciences, Shanghai 200031, China. [2]University of Chinese Academy of Sciences, Beijing 100049, China.
*These authors contributed equally to this work. †Present address: Friedrich Miescher Institute for Biomedical Research, Maulbeerstrasse 66, 4058 Basel, Switzerland. ‡Corresponding author.
E-mail: tonylicy@ion.ac.cn

measurements were used to ensure minimal residual odor in the construction of the olfactometry system (fig. S6A). In addition, a behavioral control experiment (nonmatch to long duration sample, NMLS) was performed to further exclude possible involvement of residual odor undetectable by PID. In this task, odor samples were provided during a period corresponding to the delay period in the standard DNMS task to simulate potential delay-period residual odor (fig. S6B). The sample concentration for the chance level performance of the NMLS task was well above the PID-detected residual level during the delay period in the standard DNMS task (fig. S6C).

We then suppressed the delay-period activity of pyramidal neurons with optogenetic methods. It was first achieved through activating γ-aminobutyric acid–releasing (GABAergic) inhibitory neurons expressed with channel rhodopsin (ChR2). We stereotactically and bilaterally injected AAV carrying a Cre-inducible gene encoding ChR2 [pAAV-Ef1a-DIO-ChR2(H134R)-mCherry (*21*); referred hereafter as DIO-ChR2] or mCherry (pAAV-Ef1a-DIO-mCherry, hereafter DIO-mCherry) into mPFC of vesicular GABA transporter (VGAT)–Cre transgenic mice (*23*). Expression and activity-suppression efficiency were verified by immunostaining and op-tetrode recording (fig. S7 and Fig. 2B). Optogenetic manipulation could influence neurons within 1.4 mm from an optical fiber (fig. S8) and affect all subregions of mPFC (fig. S7). Behavioral and optogenetic experiments were performed in a blind design. Step laser illumination (473 nm, 2 mW) was applied in the last 4 s of the 5-s delay period in all trials throughout the learning (Fig. 2A). Suppressing the delay-period activity of mPFC pyramidal neurons in the learning phase impaired behavioral performance, as manifested by the deficits in performance, correct rejection rate, *d'*, lick efficiency, number of trials to criterion (performance above 80% for consecutive 40 trials), and consecutive false choice (Fig. 2, A and B; figs. S9 and S10; and table S2), but not hit rate (Fig. 2B). Optogenetic suppression of mPFC delay-period activity failed to impair WM performance in well-trained mice (based on the averaged results from day 8, Fig. 2, A and B, and table S2), although session-based analysis revealed a small degree of relearning at the initial sessions, which was significantly influenced by suppressing delay-period activity (fig. S11). The results were consistent with the suggested role of PFC in performing novel and attention-demanding, rather than routine and well-rehearsed, tasks (*2*, *3*, *12*, *24*).

To directly suppress activity of mPFC pyramidal neurons, we expressed halo-rhodopsin (NpHR) (*21*) or enhanced yellow fluorescent protein (eYFP) in pyramidal neurons by injecting AAV-CaMKIIα-eNpHR3.0-eYFP or AAV-CaMKIIα-eYFP into mPFC. The expression and functionality of NpHR were verified by immunostaining and op-tetrode recording (fig. S12 and Fig. 2D). Direct suppression of delay-period activity of pyramidal neurons in mPFC by step laser illumination (532 nm, 10 mW) impaired WM performance during the learning phase but not after the mice were well trained (Fig. 2, C and D; figs. S13 and S14; and table S3).

To examine whether optogenetic manipulation influenced WM on a trial-by-trial basis, we suppressed mPFC delay-period activity in an interleaved laser on/off design (Fig. 2E). Performance was indeed impaired in laser-on trials (Fig. 2, E and F; fig. S15; and table S4). To examine the regional specificity of the behavioral effects of optogenetic manipulation, we suppressed delay-period activity in somatosensory cortex (S1) and found no impairment in WM performance (fig. S16).

To further determine whether elevating activity of mPFC pyramidal neurons during the delay period could affect the learning of a WM task, we expressed AAV-CaMKIIα-ChR2-mCherry or AAV-CaMKIIα-mCherry in mPFC of wild-type mice (Fig. 3A and fig. S17). We then applied step laser illumination (473 nm, 0.8 mW) throughout learning. When optogenetic activation was performed during the learning phase, CaMKIIα-ChR2 mice performed worse than the control group (Fig. 3A and table S5). Both hit and correct rejection rates were modulated (Fig. 3B). By contrast, optogenetic activation during the well-trained phase had no effect on the performance, although the correct rejection rate was significantly decreased. Similar results were obtained by enhancing mPFC

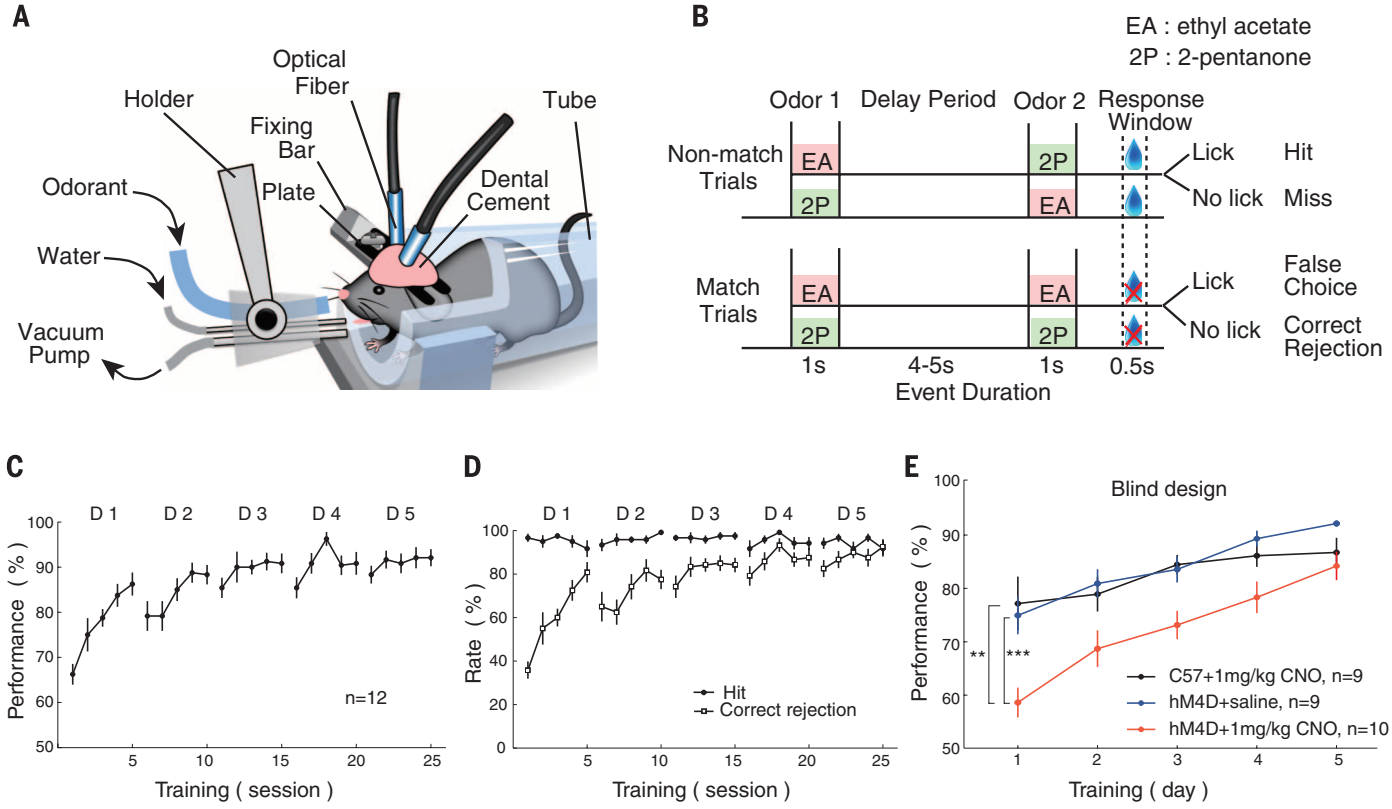

Fig. 1. WM paradigm. (**A** and **B**) Behavioral diagram. (**C**) Performance during learning. Five sessions per day, 20 trials per session. Error bars indicate SEM unless stated otherwise. (**D**) Hit rates and correct rejection rates in learning. (**E**) Performance in experiments of suppressing mPFC activity by hM4Di. $^{**}P$ = 0.003; $^{***}P < 0.001$; two-way analysis of variance with mixed design (Tw-ANOVA-md).

delay-period activity with laser illumination in an odor-sample specific manner (fig. S18). Thus, elevating mPFC activity during the delay period interfered with the learning of the WM task.

In further experiments, we suppressed mPFC activity through NpHR in the second odor-delivery period, during which decision-making behavior occurred. Behavioral performance was unaffected early in learning (days 1 and 2) but was impaired after day 3 (fig. S19). Therefore, the contribution of mPFC delay-period activity in learning of the WM task was temporally specific, a result distinct from but not contradictory to the previous findings of behavioral deficits in well-trained subjects using classic techniques to perturb mPFC activity (*3*, *15*).

To study the functional specificity of optogenetic manipulation, we used behavioral experiments of a nonmatch to sample task without the delay period (NMS-WD, Fig. 3C) and a go/no-go odor discrimination task (GNG, Fig. 3E). Both tasks required sensory encoding, inhibitory control, decision-making, and motor selection (fig. S20A) but not memory retention. In the NMS-WD task, laser illumination covered the entire period for odor perception, decision-making, and motor selection (Fig. 3C). In the GNG task with random intertrial intervals, laser illumination was applied after a trial-starting cue and before the decision-making behavior occurred (Fig. 3E),

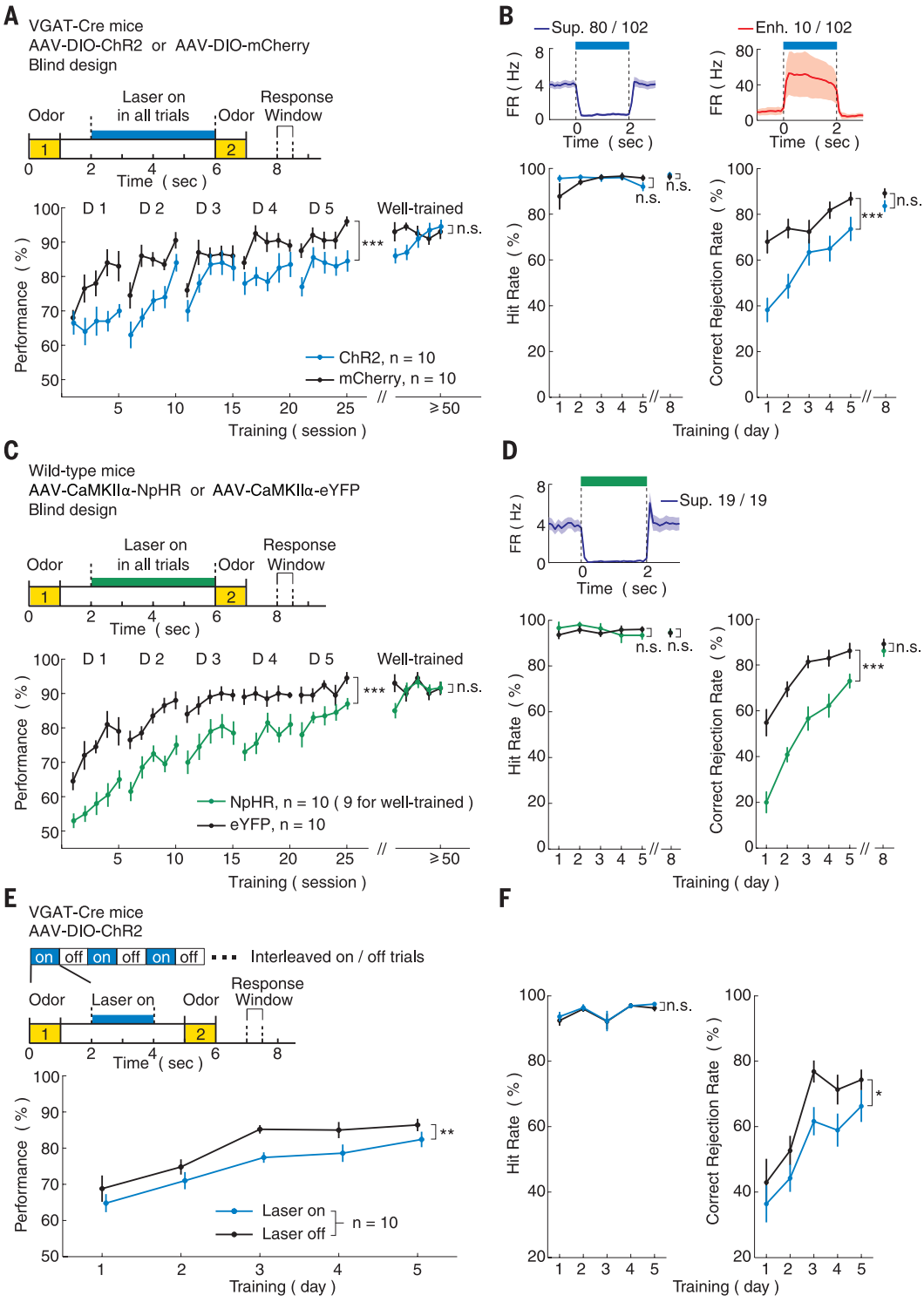

Fig. 2. Suppressing mPFC delay-period activity impaired performance in learning of the WM task. (**A** and **B**) Performance, hit rates, and correct rejection rates for experiments, in which activity of pyramidal neurons was suppressed by activating GABAergic neurons. Top in (A): paradigm information. Top in (B): activity-suppression efficiency revealed by awake op-tetrode recording in vivo. FR, firing rate. (**C** and **D**) As in (A) and (B) with NpHR in pyramidal neurons. (**E** and **F**) As in (A) and (B) with interleaved laser on/off design. *P = 0.016; **P = 0.003; ***P < 0.001; n.s., not significant; learning: Tw-ANOVA-md; well-trained: Mann-Whitney U test.

simulating the delay period in the DNMS task (fig. S20B). We found that behavioral performance was not affected by laser illumination in all trials, in either the NMS-WD (Fig. 3, C and D, and table S6) or GNG (Fig. 3, E and F, and table S7) task. In separate sets of experiments with an interleaved laser on/off design, the same results were obtained (figs. S21 and S22). Therefore, mPFC delay-period activity appeared to be more important in memory retention than sensory encoding, inhibitory control, decision-making, and motor selection.

To examine the neural correlates throughout learning the WM task, we recorded single-unit activity of mPFC by using custom-made tetrodes (Fig. 4, A to C, and figs. S23 and S24). By lowering recording electrodes each day, we recorded 564 neurons during the learning phase (days 1 to 5) from 15 mice and 95 neurons from seven well-trained (days 10 to 15) mice. Similar results were obtained from 636 neurons of nine mice without daily lowering of electrodes (figs. S25 to S28). The delay-period activity was more prominently modulated during the learning than the well-trained phase (Fig. 4D and fig. S29). The delay-period firing rates during the learning phase were significantly higher for neurons with enhanced delay-period activity and lower for suppressed neurons, as compared with those in the well-trained phase (Fig. 4E and table S8).

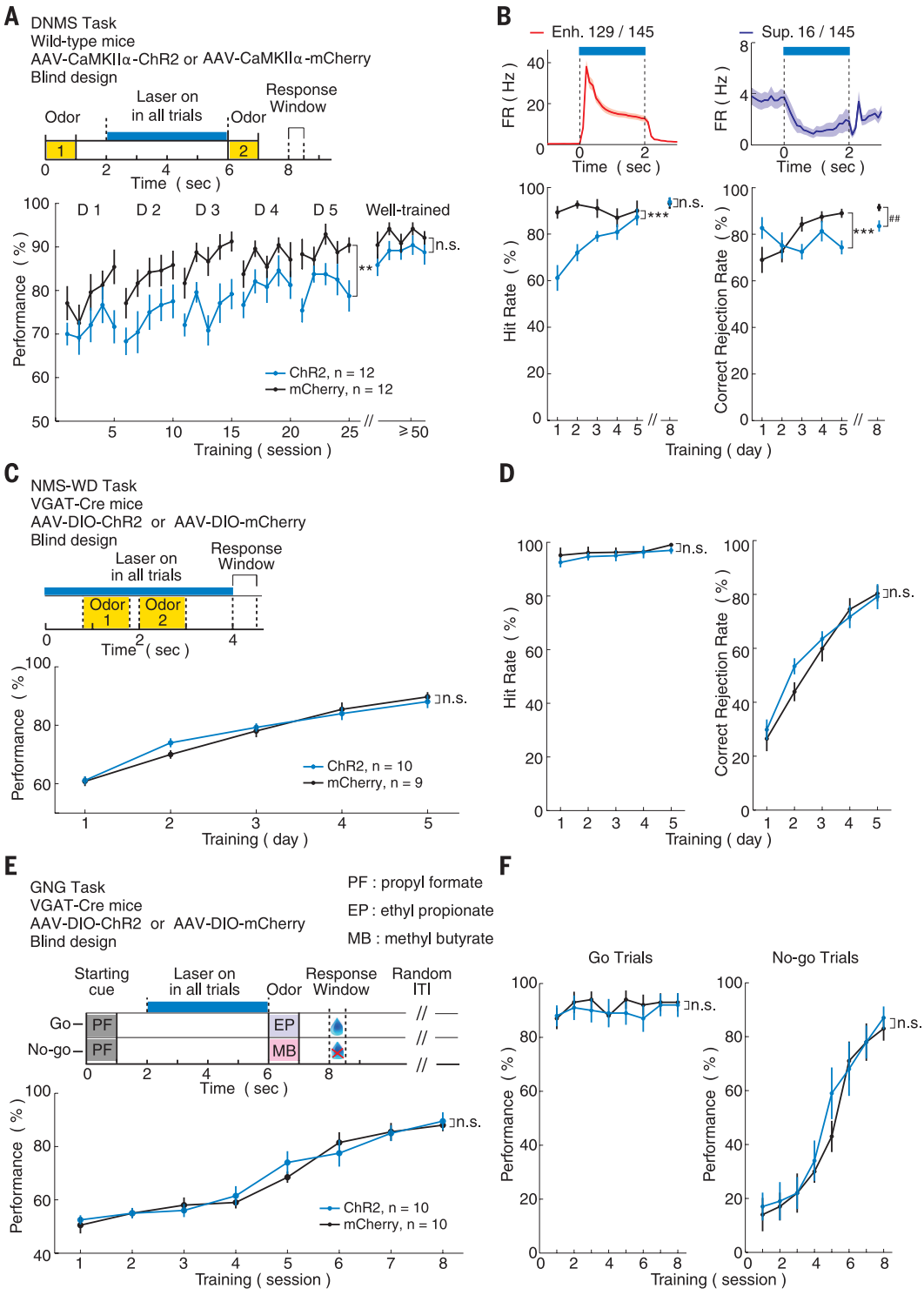

Fig. 3. Importance of properly regulated mPFC delay-period activity and its functional role in the WM task. (**A** and **B**) Performance, hit rates, and correct rejection rates in experiments with elevated mPFC activity during the delay period. (**C** and **D**) Paradigm and performance for NMS-WD experiments with suppressed mPFC activity. (**E** and **F**) As in (C) and (D) for the GNG task. $^{**}P = 0.002$; $^{***}P < 0.0001$; learning: Tw-ANOVA-md. $^{\#\#}P = 0.0048$; well-trained: Mann-Whitney U test.

To retain odor-related information, delay-period population activity should be different after distinct odor samples. We therefore visualized population activity by principal component analysis (PCA) (*25*). The first three PCs captured the majority of variance (72%). The trajectories during the delay period after two different odor samples were separated during the learning but not the well-trained phase (Fig. 4F, fig. S30, and movie S2), as quantified by the trajectory distance (Fig. 4G). The results remained robust by only using half of the neurons (fig. S31). We further analyzed the sensitivity of delay-period population trajectories to behavioral outcome and found that trajectories in correct trials were more separated than in error trials during the learning but not well-trained phase (fig. S32). In decoding analysis (*26*), delay-period activity

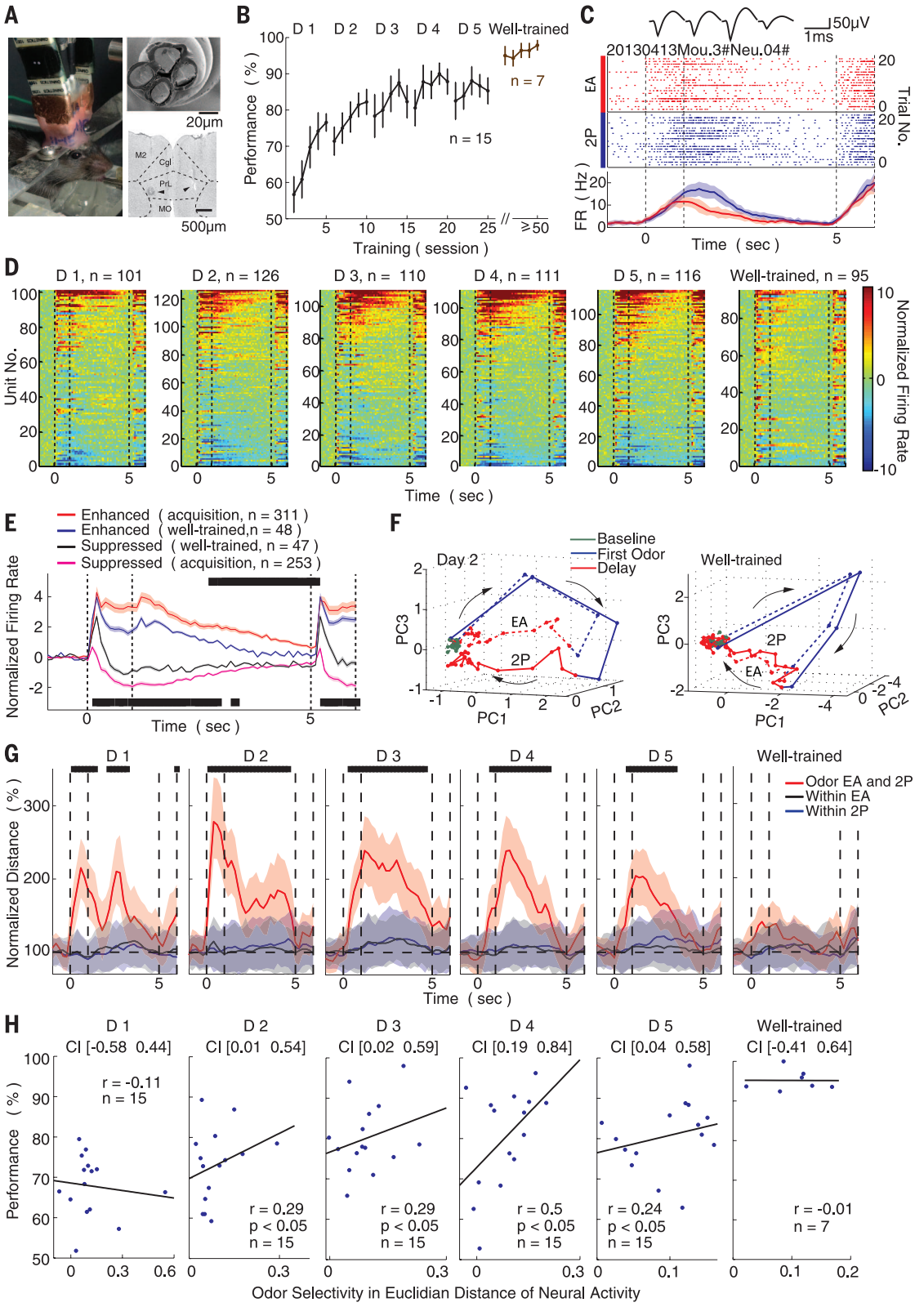

Fig. 4. Modulation of mPFC delay-period activity in learning the WM task. (**A**) Images of microdrive (left), tetrode (right top, electron microscopy), and recording sites (right bottom, indicated by arrowheads). M2, secondary motor area; Cg1, cingulate cortex, area 1; PrL, prelimbic cortex; MO, medial orbital cortex. (**B**) Performance for the recorded mice, 40 trials per session. (**C**) Spike-raster and peristimulus time histogram of an example neuron; trials sorted by odor samples. (Top) Spike waveforms. Shadows indicate SEM. (**D**) Modulation of population activity, which was normalized in *Z*-score and averaged across all trials for each neuron. Results from all the mice recorded with daily lowering of electrodes were presented in (D) to (H). (**E**) Averaged firing rates for neurons with enhanced and suppressed delay-period activity (bin of 100 ms). Black blocks indicate bins with enhanced delay-period activity and significant difference between learning and well-trained phases, $P < 0.05$, Mann-Whitney U test. Black blocks below indicate significant bins for neurons with decreased delay-period activity. Shadows, SEM. (**F**) PCA trajectories of population activity after different odor samples (bin of 200 ms). Arrows: time. (**G**) Distance in PCA trajectories. Shadows indicate 95% confidence interval (CI) from bootstrap of 100 times. (**H**) Correlations between behavioral performance and neuronal odor selectivity. Each dot represents averaged results from one mouse. Statistics: 95% CI from bootstrap of 100 times.

during the learning phase exhibited higher decoding power for odor samples than in the well-trained phase (fig. S33), which critically depended on the neurons with significant delay-period activity (fig. S34).

We then analyzed whether the delay-period odor selectivity of neurons is correlated with the behavioral performance of mice. The Euclidean distance between delay-period activity after different odor samples was calculated for a given neuron and then averaged for all neurons simultaneously recorded to represent neuronal selectivity for each mouse in one day. Although only 2 to 13 neurons (median of 8) were simultaneously recorded each day from a mouse, significant correlation between behavioral performance and neuronal selectivity was observed during the learning (days 2 to 5) but not well-trained phase (Fig. 4H and fig. S35).

The importance of mPFC delay-period activity in the learning phase of a WM task is consistent with its central role in flexible cognitive control in changing environments (*2*, *3*, *12*). However, the DL-PFC activity in primates is important in WM tasks after subjects are well trained (*3*, *12*). Because mPFC appeared earlier than DL-PFC during evolution (*12*), the functional difference between mPFC and DL-PFC suggests that memory retention in novel situations may represent an evolutionarily more primitive function. It is not clear which brain region in rodents is homologous or analogous to DL-PFC in primates (*3*, *12*), but delay-period activity in brain regions other than mPFC (*3*, *5*, *19*, *27–30*) could mediate WM in well-trained mice. Activity of mPFC in other periods during the behavioral task may underlie inhibitory control (*14*), decision-making (*15*), and motor selection (*16*). Nevertheless, the present finding underscores the notion that properly regulated delay-period activity of mPFC is critical for memory retention in attention-demanding WM tasks in novel situations.

REFERENCES AND NOTES

1. A. D. Baddeley, *Working Memory* (Oxford Univ. Press, Oxford, 1986).
2. E. K. Miller, J. D. Cohen, *Annu. Rev. Neurosci.* **24**, 167–202 (2001).
3. J. M. Fuster, *The Prefrontal Cortex* (Academic Press, London, ed. 4, 2008).
4. J. M. Fuster, G. E. Alexander, *Science* **173**, 652–654 (1971).
5. E. K. Miller, C. A. Erickson, R. Desimone, *J. Neurosci.* **16**, 5154–5167 (1996).
6. R. Romo, C. D. Brody, A. Hernández, L. Lemus, *Nature* **399**, 470–473 (1999).
7. E. H. Baeg *et al*., *Neuron* **40**, 177–188 (2003).
8. S. Fujisawa, A. Amarasingham, M. T. Harrison, G. Buzsáki, *Nat. Neurosci.* **11**, 823–833 (2008).
9. J. C. Erlich, M. Bialek, C. D. Brody, *Neuron* **72**, 330–343 (2011).
10. E. M. Meyers, X. L. Qi, C. Constantinidis, *Proc. Natl. Acad. Sci. U.S.A.* **109**, 4651–4656 (2012).
11. R. Desimone, *Proc. Natl. Acad. Sci. U.S.A.* **93**, 13494–13499 (1996).
12. R. E. Passingham, S. P. Wise, *The Neurobiology of the Prefrontal Cortex: Anatomy, Evolution, and the Origin of Insight* (Oxford Univ. Press, Oxford, ed. 1, 2012).
13. S. H. Wang, R. G. Morris, *Annu. Rev. Psychol.* **61**, 49–79, C1–C4 (2010).
14. R. Dias, J. P. Aggleton, *Eur. J. Neurosci.* **12**, 4457–4466 (2000).
15. D. R. Euston, A. J. Gruber, B. L. McNaughton, *Neuron* **76**, 1057–1070 (2012).
16. K. Matsumoto, W. Suzuki, K. Tanaka, *Science* **301**, 229–232 (2003).
17. E. A. Allen, B. N. Pasley, T. Duong, R. D. Freeman, *Science* **317**, 1918–1921 (2007).
18. S. Sobotka, M. D. Diltz, J. L. Ringo, *J. Neurophysiol.* **93**, 128–136 (2005).
19. T. Otto, H. Eichenbaum, *Hippocampus* **2**, 323–334 (1992).
20. X.-C. M. Lu, B. M. Slotnick, A. M. Silberberg, *Physiol. Behav.* **53**, 795–804 (1993).
21. L. Fenno, O. Yizhar, K. Deisseroth, *Annu. Rev. Neurosci.* **34**, 389–412 (2011).
22. B. N. Armbruster, X. Li, M. H. Pausch, S. Herlitze, B. L. Roth, *Proc. Natl. Acad. Sci. U.S.A.* **104**, 5163–5168 (2007).
23. H. T. Chao *et al*., *Nature* **468**, 263–269 (2010).
24. S. B. Ostlund, B. W. Balleine, *J. Neurosci.* **25**, 7763–7770 (2005).
25. M. Rabinovich, R. Huerta, G. Laurent, *Science* **321**, 48–50 (2008).
26. E. M. Meyers, D. J. Freedman, G. Kreiman, E. K. Miller, T. Poggio, *J. Neurophysiol.* **100**, 1407–1419 (2008).
27. M. Stopfer, G. Laurent, *Nature* **402**, 664–668 (1999).
28. C. D. Harvey, P. Coen, D. W. Tank, *Nature* **484**, 62–68 (2012).
29. Z. V. Guo *et al*., *Neuron* **81**, 179–194 (2014).
30. J. Yamamoto, J. Suh, D. Takeuchi, S. Tonegawa, *Cell* **157**, 845–857 (2014).

ACKNOWLEDGMENTS

We thank M. P. Stryker for communication on head-fixed mice preparation; Z. F. Mainen and N. Uchida for communication on behavioral design; G. Laurent for communication on population analysis; L. P. Wang for help in optogenetics; L. N. Lin for help in tetrode drive manufacturing; H. L. Hu for help in electrophysiological recordings; Y. Dan and J. F. Erlich for communication on spike sorting; H. Y. Zoghbi for VGAT-Cre mice; B. L. Roth for DREADD vectors; Z. L. Qiu, H. L. Hu, and X. Yu for help on AAV virus packaging and transgenic mice; A. K. Guo for help in PID experiments; Q. Hu for help in imaging experiments; Y. G. Sun for histochemistry experiments; Y. F. Li for help in drawing diagrams; and M. M. Poo and R. Desimone for critical comments on the manuscript. The work was supported by Chinese 973 Program (2011CBA00406), the State Key Laboratory of Neuroscience, and Chinese Academy of Sciences Hundreds of Talents Program (to C.T.L.). All the behavioral, optogenetic, electrophysiological, and histochemical data are archived in Institute of Neuroscience, Shanghai Institutes for Biological Sciences, Chinese Academy of Sciences.

SUPPLEMENTARY MATERIALS

www.sciencemag.org/content/346/6208/458/suppl/DC1
Materials and Methods
Figs. S1 to S35
Tables S1 to S8
References (*31–42*)
Movies S1 and S2

27 May 2014; accepted 16 September 2014
10.1126/science.1256573

EVOLUTIONARY BIOLOGY

Rapid evolution of a native species following invasion by a congener

Y. E. Stuart,[1]*†‡ T. S. Campbell,[2]* P. A. Hohenlohe,[3] R. G. Reynolds,[1,4] L. J. Revell,[4] J. B. Losos[1]

In recent years, biologists have increasingly recognized that evolutionary change can occur rapidly when natural selection is strong; thus, real-time studies of evolution can be used to test classic evolutionary hypotheses directly. One such hypothesis is that negative interactions between closely related species can drive phenotypic divergence. Such divergence is thought to be ubiquitous, though well-documented cases are surprisingly rare. On small islands in Florida, we found that the lizard *Anolis carolinensis* moved to higher perches following invasion by *Anolis sagrei* and, in response, adaptively evolved larger toepads after only 20 generations. These results illustrate that interspecific interactions between closely related species can drive evolutionary change on observable time scales.

In their classic paper, Brown and Wilson (*1*) proposed that mutually negative interactions between closely related species could lead to evolutionary divergence when those species co-occurred. In the six decades since, this idea has been debated vigorously, with support that has vacillated, depending on the latest set of theoretical treatments and comparative studies [reviewed in (*2–5*)]. However, tests of interaction-driven evolutionary divergence have been slow to capitalize on the growing recognition that evolutionary change can occur rapidly in response to strong divergent natural selection [but see (*6–9*)]; thus, evolutionary hypotheses about phenomena once thought to transpire on time scales too long for direct observation can be tested in real time while using replicated statistical designs.

An opportunity to study such real-time divergence between negatively interacting species has been provided by the recent invasion of the Cuban brown anole lizard, *Anolis sagrei*, into the southeastern United States, where *Anolis carolinensis* is the sole native anole. These species have potential to interact strongly [e.g., (*10*)], being very similar in habitat use and ecology (*11*). We investigated the eco-evolutionary consequences of this interaction on islands in Florida (*12*) using an *A. sagrei* introduction experiment, well-documented natural invasions by *A. sagrei*, genomic analyses of population structure, and a common garden experiment. This multifaceted approach can rule against several of the most

[1]Museum of Comparative Zoology and Department of Organismic and Evolutionary Biology, Harvard University, Cambridge, MA, USA. [2]Department of Biology, University of Tampa, Tampa, FL, USA. [3]Department of Biological Sciences and Institute for Bioinformatics and Evolutionary Studies, University of Idaho, Moscow, ID, USA. [4]Department of Biology, University of Massachusetts, Boston, MA, USA.
*These authors contributed equally to this work. **†Corresponding author. E-mail: yestuart@utexas.edu** ‡Present address: Department of Integrative Biology, University of Texas, Austin, TX, USA.